

---

## Geotechnical characterization of tropical soil via laboratory testing

### Caracterização geotécnica de solo tropical a partir de ensaios de laboratório

Received: 21-07-2024 | Accepted: 25-08-2024 | Published: 31-08-2024

---

#### **Fernando Feitosa Monteiro**

ORCID: <https://orcid.org/0000-0002-4451-4623>

State University of Campinas, Brazil

E-mail: [feitosam@unicamp.br](mailto:feitosam@unicamp.br)

#### **Paulo José Rocha de Albuquerque**

ORCID: <https://orcid.org/0000-0003-0726-7165>

State University of Campinas, Brazil

E-mail: [pjra@unicamp.br](mailto:pjra@unicamp.br)

#### **Fernanda dos Santos Gon Gliotti**

ORCID: <https://orcid.org/0009-0008-5917-9080>

State University of Campinas, Brazil

E-mail: [fernandagon86@gmail.com](mailto:fernandagon86@gmail.com)

---

### ABSTRACT

This manuscript presents the evaluation of relevant geotechnical properties of the soil profile in the northern region of Campinas, which are important for geotechnical engineering practice and development in São Paulo State. Disturbed and undisturbed samples from the subsoil were collected through the excavation of inspection shafts at the experimental site for Soil Mechanics and Foundations research at the State University of Campinas, located at the Faculty of Civil Engineering, Architecture and Urbanism (FEC). Laboratory tests were conducted, including soil characterization, soil shear strength, soil compressibility, soil permeability, and soil suction tests. The characterization tests indicated that the upper soil layer is subject to surface effects and more direct weathering action, with noticeable variations in the liquid and plasticity limit values. The permeability test results showed no significant variation between the values obtained in the vertical and horizontal directions. The soil-water characteristic curves for the studied profile were bimodal, typical of tropical soils with macro and microaggregated structures.

**Keywords:** Geotechnical characterization; Laboratory tests; Diabase residual soil;

---

### RESUMO

Este artigo apresenta a avaliação de propriedades geotécnicas relevantes do perfil do solo de Campinas, que são importantes para a prática e desenvolvimento da engenharia geotécnica no Estado de São Paulo. Amostras deformadas e indeformadas do subsolo foram coletadas a partir da escavação de poços de inspeção no campo experimental de Mecânica dos Solos e Fundações da Universidade Estadual de Campinas, localizado na Faculdade de Engenharia Civil, Arquitetura e Urbanismo (FEC). Foram realizados ensaios de laboratório, incluindo caracterização do solo, resistência ao cisalhamento do solo, compressibilidade do solo, permeabilidade do solo e ensaios de papel filtro. Os ensaios de caracterização indicaram que a camada superior do solo está sujeita a efeitos da superfície e a uma ação mais direta do intemperismo, com variações notáveis nos valores dos limites de liquidez e plasticidade. Os resultados dos ensaios de permeabilidade não mostraram variação significativa entre os valores obtidos nas direções vertical e horizontal. As curvas de retenção de água do solo para o perfil estudado foram bimodais, típicas de solos tropicais com estruturas macro e microagregadas.

**Palavras-chave:** Caracterização geotécnica; Ensaios de laboratório; Solo residual de diabásio;

---

## INTRODUCTION

The successful implementation of engineering projects necessitates a preliminary characterization of the soil that will support the construction. The primary objective of an adequate geotechnical investigation is to delineate the subsoil stratigraphy and obtain relevant soil parameters for behavioral predictions. The use of experimental fields dedicated to geotechnical research is highly beneficial, as the accumulated data from these fields facilitate the advancement of applied research. Many scientific studies on the characterization of Geotechnical Experimental Fields are available in the literature (Albuquerque et al. 2006; Cortizo et al. 2011; Gon, 2011; Rocha and Giacheti, 2018; Dos Santos and Coutinho, 2023; Baldovino et al. 2024). For instance, Cavalcante et al. (2006) presented a comprehensive overview of the geotechnical aspects of Geotechnical and Foundation Experimental Fields across 11 locations in Brazil, all situated within federal and state universities. The investigations conducted in these subsoils have significantly contributed to the research developed in dissertations, theses, and scientific publications, providing a robust foundation for ongoing and future geotechnical studies (Moura et al. 2021).

Moreover, few studies have focussed on the geotechnical characterization of campinas diabase residual soil. Exploration and extraction of significant subsurface parameters are essential in complex geotechnical circumstances for offering practical applications and insights for ongoing and upcoming projects. This paper aims to assess the geotechnical properties of the northern Campinas soil profile, which are relevant to the practice and development of geotechnical engineering in São Paulo State.

## GENERAL CHARACTERISTICS OF THE STUDY AREA

The research was conducted at the new experimental area (20 m x 30 m) for soil mechanics and foundations studies at the State University of Campinas (Campinas Campus), located at the Faculty of Civil Engineering, Architecture, and Urbanism (FEC) in Southern Brazil (Figure 1). A shaft was excavated at the site to collect undisturbed samples up to 8 m deep and disturbed samples up to 9 m deep. Beyond this depth, it was no longer possible to collect samples due to the presence of large boulders. Using the extracted samples, a series of characterization, permeability, consolidation, triaxial, and compaction tests were initiated.

**Figure 1** – Map of São Paulo State in Brazil showing the location of the cities



Source: Garcia and Albuquerque (2019)

The subsoil of the region is composed of basic magmatites, with the presence of basic intrusive rocks (Diabases) from the Serra Geral Formation, which is part of the São Bento Group. These rocks cover 98 km<sup>2</sup> of the Campinas region, occupying 14% of the total area. The profile of the experimental field consists of diabase soil with an approximately 6 m thick surface layer of colluvial origin, characteristic of 14% of the Campinas region. This layer is composed of a silty-sandy clay with high porosity, of lateritic and collapsible origin. Beneath it, there is a saprolitic soil layer of silty-sandy clay extending to a depth of 20 meters. The water table is approximately at 17 meters (Zuquette, 1987).

From a geotechnical perspective, the surface layer is predominantly composed of secondary or transformed minerals, including clay minerals, iron oxides and hydroxides, manganese, titanium, and occasionally aluminum, and is classified as mature soil. The subsurface layer, which still retains features inherited from the parent rock, is identified as young residual soil, saprolitic soil, or saprolite. Beneath this layer is the weathered rock, characterized by minerals exhibiting clear signs of alteration, such as the loss of luster and color.

## MATERIALS AND METHODS

Initially, a shaft with an 0.8 m diameter was excavated to retrieve the samples. The first 0.5 m of depth excavated were discarded, and from that point, samples were

collected every meter of excavation. At the time of collection, the soil moisture content was determined using the oven dry test, standardized by ABNT (1986b). The disturbed samples, after being collected, were identified and stored in hermetically sealed plastic bags to prevent moisture loss in the Soil Mechanics Laboratory at UNICAMP, awaiting characterization tests. The undisturbed blocks were collected with approximate dimensions of 0.25 m x 0.25 m x 0.25 m, following the recommendations of ABNT (1986a). All the blocks were collected, taken to the surface, and then transported as quickly as possible to the laboratory to prevent moisture loss. The blocks were unmolded on a wooden plate and then paraffined. After that, they were covered with an open mesh fabric and paraffined again. The blocks were stored in a humid environment to prevent moisture gain or loss, before being used in tests. Figure 2 depicts the sampling of the undisturbed block from the first meter of excavation. A total of nine disturbed soil samples and eight undisturbed blocks were collected.

**Figure 2** – Excavation of soil block from sampling site



Source: The authors (2024)

Disturbed samples were collected and prepared in accordance with the ABNT (1986b) standard to perform traditional geotechnical characterization tests, such as particle size analysis, Atterberg limits, and grain density. Soil particle size analysis involved two stages: sieving and sedimentation, and it was performed in accordance with the ABNT (1984a). The liquid limit and plastic limit tests, which are part of the Atterberg limits tests, were carried out in compliance with the requirements of ABNT (1984b) and ABNT (1984c), respectively. In accordance with the ABNT (1984d), the pycnometer method was used to determine the specific gravity of soil particles.

Oedometer tests were conducted using a load application system and consolidation cell assembly for all depths of the profile. Each specimen was tested

according to the ABNT (1990), up to a predetermined stress level. Subsequently, flooding was carried out, and additional deformations (collapse) were measured until complete stabilization. The test then continued for other loadings with the specimen under flooded conditions. The stages of flooding stress were 100, 200, and 400 kPa, aiming to obtain the structural collapse coefficients and identify the stress range that would cause significant additional settlements (collapses), considering the most commonly used stages in foundation engineering practice. At the end of each test, the specimen was unloaded through at least three unloading stages. From this laboratory consolidation test, pre-consolidation stress ( $\sigma'_a$ ), compression and recompression indexes ( $C_c$ ,  $C_r$ ) were obtained. The preconsolidation stress ( $\sigma'_a$ ) was determined using the graphical methods of Pacheco Silva and Casagrande.

Undisturbed samples were subjected to consolidated undrained triaxial compression tests at natural moisture content, following the procedures prescribed by Head (1986). The specimens were subjected to confining pressure and then to axial loading without allowing drainage, thus the test was interpreted in terms of total stresses. The triaxial tests were conducted with confining stress values both above and below the average preconsolidation stress obtained. Therefore, four specimens were used for each depth: two for confining stresses prior to preconsolidation stress and two for postconsolidation stresses, allowing two stress circles to be obtained before and after this value for all depths, totaling 32 specimens. The confining pressures ( $\sigma_3$ ) used in all tests were 50, 100, 300, and 400 kPa, with the preconsolidation stress being approximately 200 kPa.

The samples were subjected to hydraulic conductivity ( $k$ ) tests in the laboratory using a variable head permeameter, according to the recommendations of ABNT (2000). For each depth, two cylindrical specimens were molded: one for the determination of vertical hydraulic conductivity and the other for horizontal hydraulic conductivity. Time readings were taken at initial and final head intervals with  $h_0 = 74.4$  cm and  $h_f = 64.4$  cm. A detailed description of this test and the various factors affecting the results can be found in Head (1986). In this test, distilled and deaerated water is used and percolated through the specimen for saturation. Subsequently, the amount of water flowing through the specimen is determined by measuring the time interval for changes in the water level. The tests were conducted by molding the specimens with approximately 15 cm in height and 8 cm in diameter from undisturbed samples. After determining the geometry and mass, the specimen is placed in the permeameter, positioned in a cylinder of known dimensions

and confined between two porous plates. The discharge is measured in a graduated burette with a known section, and the time taken for the water to drop from the initial height to the final height is recorded. With these data, the permeability coefficient ( $k$ ) is calculated using Darcy's law, and the value is corrected to a temperature equivalent to 20°C ( $k_{20}$ ). Bentonite was used to seal the walls, thus preventing lateral flow.

The soil samples were air-dried, disaggregated, and sieved in the lab using a 4.76 mm mesh sieve to perform the compaction tests. According to (ABNT, 1986c), the sample was compacted using Normal Proctor energy in three soil layers and placed in a metallic cylinder with a volume of about 0.001 m<sup>3</sup>. Each layer was subjected to 26 blows from a 2.50 kg hammer that was dropped from a height of 0.305 m.

To determine the soil-water characteristic curve (SWCC), sixteen undisturbed samples were prepared. These samples, collected from various depths during the excavation of the borehole, were molded into metal rings with dimensions of 2.0 cm in height and 5.0 cm in diameter. Two samples were used for each depth. The SWCC was derived through wetting and drying processes. Initially, the samples were saturated by capillarity for 48 hours on a porous stone that had been pre-saturated with distilled water, and subsequently subjected to drying. The setup (porous stone and sample) was placed in a tray with distilled water, with the water level in the tray reaching halfway up the porous stone to ensure it remained saturated and allowed the samples to saturate by capillarity.

A filter paper was placed between the sample and the porous stone to prevent material loss. The samples were placed in a very low moisture condition, between 0 and 1%, and were wetted for 24 hours in an oven. The test was carried out in a temperature-controlled chamber at roughly 20°C. To avoid material loss during handling, filter papers were placed immediately in contact with the samples, which were fixed on the sides of the rings and coated with PVC plastic film on the bottom of the metal ring. A minor burden (the lid of an aluminum capsule) was added to guarantee that the paper made complete contact with the soil, and the arrangement was covered with aluminum foil. The entire setup was protected again with PVC plastic film and placed inside a polystyrene cooler to prevent air moisture variations from interfering with the equilibrium between the filter paper and the soil. This procedure was performed as quickly as possible to prevent the filter paper from equilibrating with the air, i.e., with the relative humidity of the air. The samples were left in the cooler for seven days to allow the equilibrium time between the filter paper and the soil to be achieved. After seven days, the samples were removed from the cooler, and the following steps were taken: the PVC plastic film and

aluminum cover were removed, along with the filter paper in contact with the soil. The filter paper was then placed into an aluminum capsule with a known mass, and the mass of the setup was determined using a scale with a precision of 0.1 mg. This procedure, from removing the protective layers to placing the filter paper in the capsule for mass determination, was completed in less than 10 seconds to avoid the filter paper gaining or losing moisture. Once weighed, the filter paper was placed in an oven for 48 hours at approximately 60°C. To determine the equilibrium moisture content values through the wetting process, a certain amount of distilled water was uniformly added to the surface of the sample using a dropper, and it was left for two hours to allow the water to infiltrate the sample, ensuring it did not accumulate on the surface. This step was then repeated.

In the drying process, the sample was placed in front of a window to allow the sun's heat to evaporate the water contained in the soil. Once the expected mass and moisture content were achieved, the filter paper placement process was repeated. At a certain moisture content, no more water could be lost by evaporation from the sample in the air, so the samples were placed in the oven for a few minutes to remove additional water. After drying the filter paper, its mass was again determined, always accounting for moisture variations. The same procedure was performed with the soil samples.

Throughout all phases of the test, the filter paper was handled with metal tweezers to avoid altering its characteristics. Equilibrium moisture contents of the filter paper and soil were determined, with each gravimetric moisture corresponding to a matric suction estimated from the filter paper moisture content using calibration curves for Whatman No. 42 paper obtained by Chandler et al. (1992). Each pair of suction and moisture content values corresponded to a point on the water retention curve. An examination was conducted to confirm the validity of the calibration curve generated by Chandler et al. (1992) for the filter paper batch utilized in the research experiments. This verification was conducted using the axis translation technique. After the porosity plate was wet and put in the Richards pressure plate device, any extra water that was left on top of it was wiped off to prevent tampering with the results by giving the filter paper more water. The paper was placed under the porous plate, and a pressure of 200 kPa was applied. The paper was taken out of the device and its moisture content was measured after a week. The paper was allowed to come into balance with the applied suction for a week within the device. The equivalent suction value was calculated using Chandler et al.'s (1992) equation and the moisture content of the paper. It was discovered that the moisture content value corresponded to a suction of 200 kPa.

**RESULTS AND DISCUSSIONS**

In Table 1, a summary of the obtained soil index properties is presented: moist unit weight ( $\gamma_n$ ), dry unit weight ( $\gamma_d$ ), unit weight of solids ( $\gamma_s$ ), water content ( $w$ ), void ratio ( $e$ ), degree of saturation ( $S_r$ ), and porosity ( $n$ ). As mentioned earlier, during the sample collection, the natural moisture content was determined using the oven drying test.

**Table 1** – Soil index properties of the experimental area

Depth (m)	$\gamma_n$ (kN/m <sup>3</sup> )	$\gamma_s$ (kN/m <sup>3</sup> )	$\gamma_d$ (kN/m <sup>3</sup> )	w (%)	e	n (%)	Sr (%)
1	14.1	30.4	11	28.3	1.77	64	48.4
2	14.2	30.8	11.1	27.9	1.78	64	48.4
3	14	30.5	10.9	28	1.79	64	47.5
4	14.4	30.6	11.5	25.5	1.68	63	46.8
5	15.5	30.4	12.3	26.2	1.51	60	53.5
6	15.3	30.4	12.2	26.1	1.47	59	53.5
7	15.4	30.4	12	28.3	1.54	61	56.1
8	15.2	29.8	11.5	32.3	1.60	62	60.4
9	15.2	29.5	10.8	40.6	1.73	63	69.2

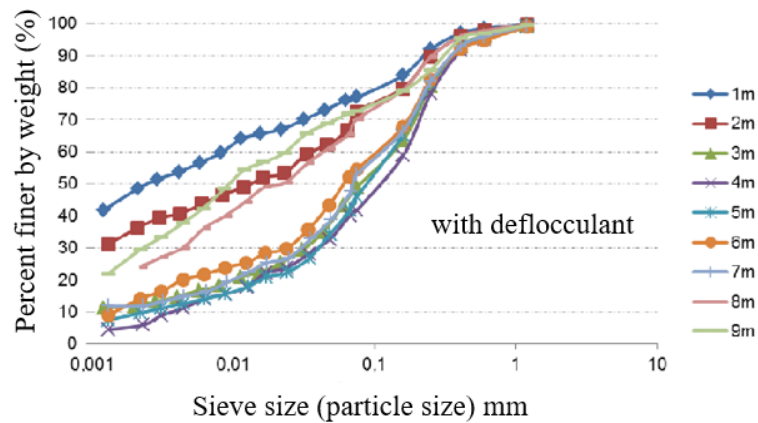
Source: The authors (2024)

Analyzing the values presented in Table 1 reveals that the samples exhibit low saturation levels and high void ratios, typical of lateritic tropical soils as reported in the literature. The relatively high unit weight of solids in the samples suggests the presence of iron oxides, which are likely cementing agents resulting from the hydrolysis processes characteristic of lateritic soils.

Figures 3 and 4 illustrate the grain size distribution curves of the soil samples tested with and without deflocculant, respectively. Sand percentages ranged from 20% to 65%, silt percentages from 25% to 45%, and clay percentages from 0% to 50%, according to the deflocculant testing. The percentages of clay decreased to 0% to 30%, silt increased to 25% to 65%, and sand ranged from 25% to 70% in the absence of deflocculant. This illustrates how soil behavior varies. Notably, the clay component exhibits a significant decrease around 4 m, followed by a subsequent increase at greater depths, although in

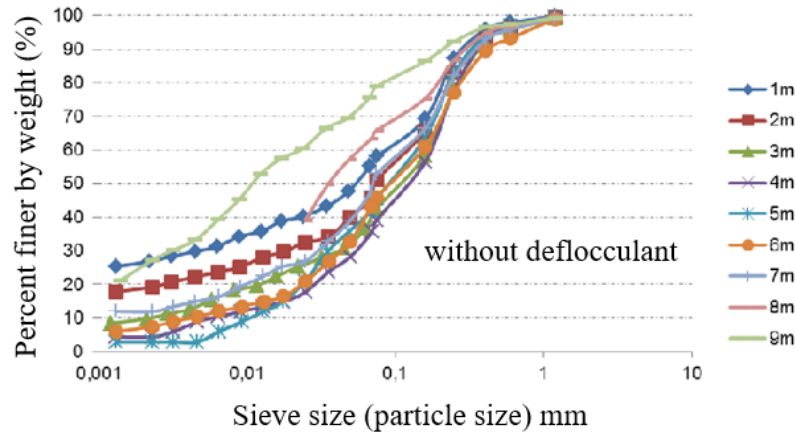
lower quantities. Additionally, it is evident that the proportion of sand increases between 3 and 7 m, although the amount of silt is mostly unchanged with a small increase in the last 2 m.

**Figure 3** – Grain size distribution curves of the soil samples tested with deflocculant



Source: The authors (2024)

**Figure 4** – Grain size distribution curves of the soil samples tested without deflocculant



Source: The authors (2024)

The grain size classifications under the influence of deflocculant indicate that the soil textures are silty-sandy clays up to a depth of 2 m, silty sands from 3 m to a depth of 8 m, and sandy-clay silts beyond that. In the case of grain size curves obtained without deflocculant, the profile consists of silty-clayey sands up to a depth of 2 m, silty sands up to a depth of 7 m, and sandy silt from there to a depth of 9 m.

The values obtained for liquid limit ( $w_L$ ), plastic limit ( $w_P$ ), shrinkage limit ( $w_S$ ), and plasticity index (PI), based on the depth at which the samples were collected, are presented in Table 2.

**Table 2** – Soil consistency limits and indexes

Depth (m)	$w_L$ (%)	$w_P$ (%)	$w_S$ (%)	PI (%)
1	50.9	30.2	20.6	20.7
2	44.3	31.8	24.4	12.5
3	44.6	33	24.9	11.6
4	44.4	32.6	25.2	11.8
5	44.8	34.2	27.8	10.6
6	44.9	37.4	29.3	7.5
7	46.2	39	31.3	7.2
8	51.4	42.4	29.6	9
9	52.2	41.3	30.4	10.9

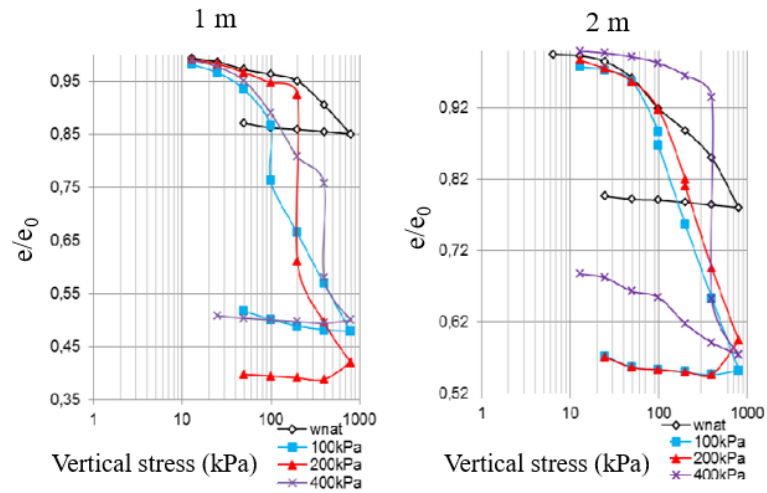
Source: The authors (2024)

It is observed that the liquid limit values are above 40% and the average plasticity index is around 10%. The shrinkage limit values varied between 20% and 30%. Notably, the values for the first meter differ from the rest of the profile, as this zone experiences significant seasonal moisture variations, leading to continuous soil contraction and expansion, which alters the material properties. Consequently, there is a noticeable variation in the curves of the liquid limit, plastic limit, and plasticity index values. Immediately after this superficial layer, there is another layer between 2 m and 7 m where the properties show less variation, particularly the liquid limit and shrinkage limit curves, which exhibit low value oscillation. Beyond this layer, a change in soil behavior is observed. This change in the soil profile occurs around 8 m in depth and was visually noted as the soil color and texture changed from dark brown to a more yellowish hue. It was possible to observe that, throughout its extent, the soil is classified as inorganic silt, with medium compressibility from 2 to 7 m depth, and high compressibility in the last meters of the profile.

Figures 5 to 8 present the soil compression curves obtained from double oedometer tests to evaluate the collapsibility of all tested samples. The deformations induced by wetting (collapse deformations) were measured under stresses of 100, 200, and 400 kPa. The void ratio values were normalized by dividing the initial void ratio by

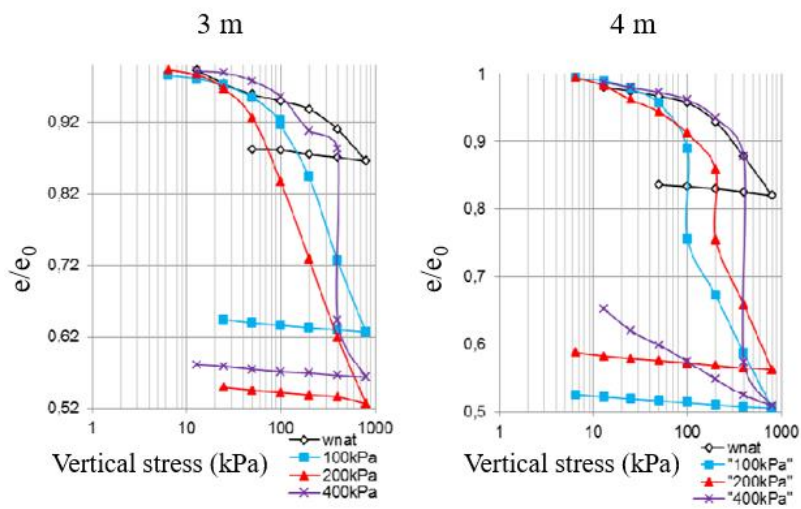
the void ratio obtained for each loading stage, enabling a comparative analysis of the different samples.

**Figure 5** –Soil compression curves obtained from double oedometer tests on samples at 1 and 2 m depth



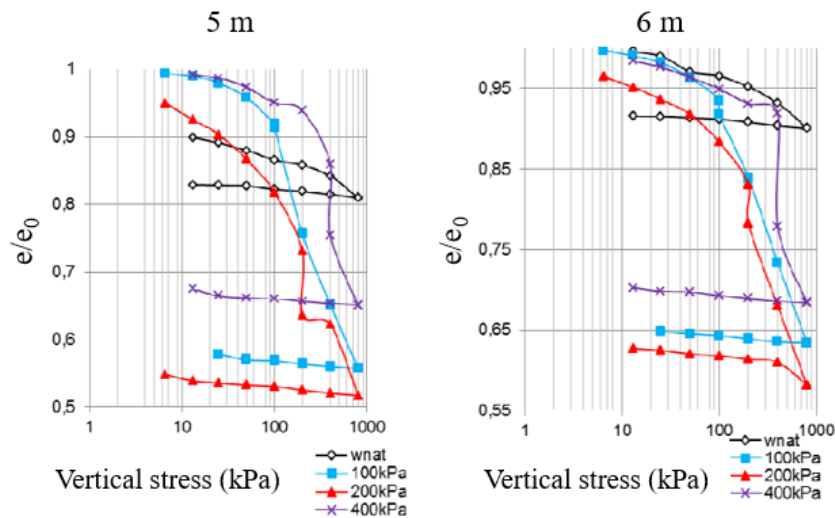
Source: The authors (2024)

**Figure 6** – Soil compression curves obtained from double oedometer tests on samples at 3 and 4 m depth



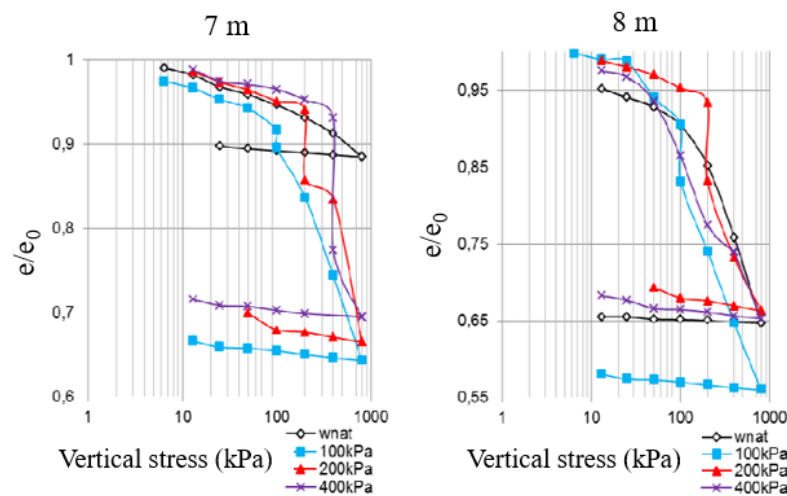
Source: The authors (2024)

**Figure 7** – Soil compression curves obtained from double oedometer tests on samples at 5 and 6 m depth



Source: The authors (2024)

**Figure 8** – Soil compression curves obtained from double oedometer tests on samples at 7 and 8 m depth



Source: The authors (2024)

The compression curves presented significant volumetric variations during floods. Substantial variances were found for the 100 kPa flooding stress only at depths of 1 and 4 m. Only 2 and 3 m depths showed slight differences in the flooding under 200 kPa stress, but all depths except 8 meters showed considerable variations in the flooding with 400 kPa stress. Using the 200 kPa flooding stress as a reference standard, the criteria of Vargas (1978) and Jennings and Knight (1975) were employed to examine the samples' collapsibility due to flooding at different loading levels. Tables 3 and 4 provide the results obtained for the collapse potential of the samples.

**Table 3** – Collapse potential (CP) according to Jennings and Knight (1975)

<b>Depth (m)</b>	<b>CP at 100 kPa (%)</b>	<b>CP at 200 kPa (%)</b>	<b>CP at 400 kPa (%)</b>
<b>1</b>	6.5	20.20	5.0
<b>2</b>	1.2	0.56	18.01
<b>3</b>	0.43	0.35	15.30
<b>4</b>	8.4	6.34	19.48
<b>5</b>	0.26	5.5	6.2
<b>6</b>	1.05	2.96	8.02
<b>7</b>	1.29	5.11	9.3
<b>8</b>	4.64	5.95	0.08

Source: The authors (2024)

**Table 4** – Collapse potential (CP) according to Vargas (1978)

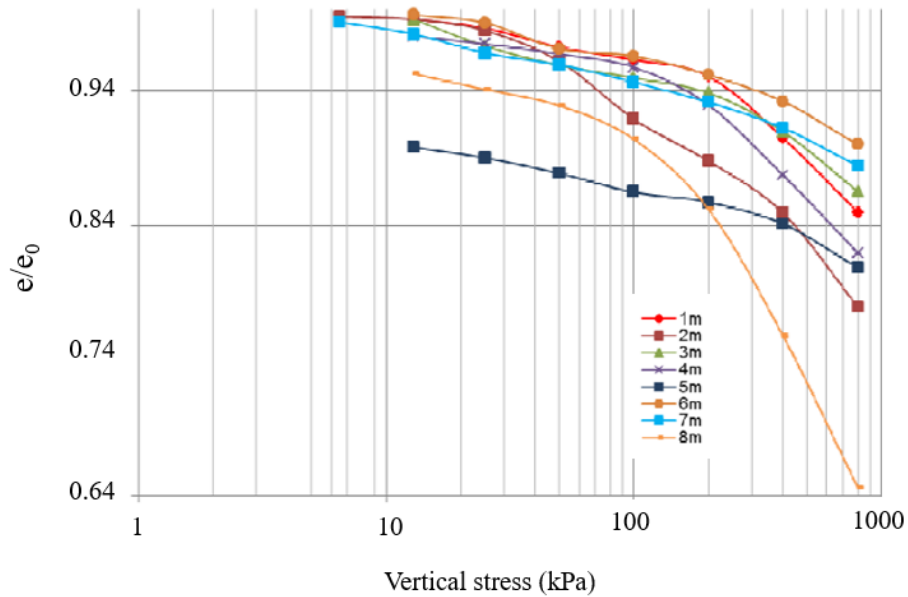
<b>Depth (m)</b>	<b>CP at 100 kPa (%)</b>	<b>CP at 200 kPa (%)</b>	<b>CP at 400 kPa (%)</b>
<b>1</b>	7.8	27	6
<b>2</b>	1.3	0.65	23
<b>3</b>	0.45	0.04	19.84
<b>4</b>	9.9	7.5	26.8
<b>5</b>	0.28	7.03	7.24
<b>6</b>	1.1	3.4	9.2
<b>7</b>	1.4	5.6	10.74
<b>8</b>	5.20	6.6	0.09

Source: The authors (2024)

The sample representative at a 1 m depth exhibited high collapsibility potential for all flooding stresses. Low collapsibility potential was observed for stresses of 100 and 200 kPa in the samples from the 2 and 3 m depth layers, whereas an elevated collapsibility potential was noted at a stress of 400 kPa. The results indicated that only the depths of 1, 4, and 8 m collapsed under a 100 kPa stress. At a 200 kPa stress, only the 2 and 3 m depth samples were not collapsible. Lastly, nearly all depths collapsed under a 400 kPa flooding stress, except for the 8 m depth sample.

Figure 9 shows the normalized compression curve of the soil in its natural condition for all depths. Table 5 presents the geostatic vertical stresses ( $\sigma'_{v0}$ ), preconsolidation stresses ( $\sigma'_a$ ), and compression and recompression indexes ( $C_c$  and  $C_r$ ) of the soil in its natural condition.

**Figure 9** – Normalized compression curve of the soil in its natural condition for all depths



Source: The authors (2024)

**Table 5** – Soil compression parameters obtained from oedometer tests

Depth (m)	$\sigma'_{v0}$ (kPa)	$\sigma'_a$ (kPa)	$C_c$	$C_r$	OCR
1	10.96	180	0.332	0.042	16.42
2	22.18	178	0.423	0.049	8.02
3	32.70	203	0.261	0.045	6.02
4	46	163	0.294	0.040	3.54
5	61.5	178	0.160	0.053	2.89
6	72.3	195	0.148	0.094	2.69
7	84	185	0.152	0.070	2.2
8	92	183	0.125	0.100	1.99

Source: The authors (2024)

It can be observed that all layers are overconsolidated since the preconsolidation stresses are greater than the existing effective vertical stresses. This indicates that the soil

profile was subjected to higher stresses in the past, likely due to the presence of an overlying soil layer or due to desiccation. From a depth of 1.2 meters, the preconsolidation stress increases, but from 3.2 meters, there is a significant decrease that continues until 4 m. Beyond this point, the preconsolidation stress increases with depth, stabilizing at approximately 7 m. The average value of the preconsolidation stress is around 180 kPa. Analyzing the obtained compression indexes ( $C_c$ ), it is noted that the value initially increases and decreases up to a depth of 4 m, and then decreases with depth. The maximum compression index value was found at a depth of 2 m. The recompression index ( $C_r$ ) values decrease with increasing depth up to 5 m, followed by a small increase and then another decrease up to a depth of 8 m.

The numerical values of cohesion intercepts and friction angles for both normally consolidated (NC) and overconsolidated (OC) portions were obtained (Table 6) for each depth from the triaxial tests performed, as detailed in the materials and methods section.

**Table 6** – Soil shear strength parameters

Depth (m)	Portion	Moisture content (%)	Cohesion intercept (kPa)	Friction angle (°)
1	OC	28.3	185	5
	NC		0	24
2	NC	27.9	0	27
3	NC	28	0	28
4	OC	25.5	141	11
	NC		0	20
5	OC	26.2	159	8
	NC		0	27
6	NC	26.1	68	19
	OC		0	33
7	NC	28.3	0	29
8	OC	32.3	79	15
	NC		0	30

Source: The authors (2024)

Testing at depths of 2, 3, and 7 m with a confining stress ( $\sigma_c$ ) of 400 kPa could not be conducted to establish the failure envelopes. Consequently, only the failure envelope

for the normally consolidated portion was obtained. This limitation resulted from the testing apparatus's inability to provide sufficient precision and the lack of additional undisturbed samples for new test specimens. For the remaining depths, soil shear strength parameters for both normally consolidated and overconsolidated portions were determined by plotting two Mohr circles with confining stresses below the preconsolidation stress and two with stresses above this value.

It was observed that the friction angle values for the normally consolidated portion exhibited minimal variation, indicating that the soil at the analyzed depths displays consistent behavior. Conversely, the overconsolidated portions showed low friction angle values. This phenomenon can be attributed to significant cementation in these samples, likely due to iron oxides. This characteristic manifest as distinct shear strength behavior during triaxial testing. When tests are conducted with confining stresses lower than the preconsolidation stress, the maximum deviatoric stress is reached with minor deformations and relatively high values, facilitating the breakdown of cementation. As a result, the Mohr circles in these scenarios have very similar radii, leading to very low friction angles and high cohesion intercepts.

Table 7 presents the results of the soil permeability tests obtained in the laboratory in both horizontal and vertical directions.

**Table 7 – Soil hydraulic conductivity**

<b>Depth (m)</b>	<b><math>k_v \times 10^{-5}</math> (m/s)</b>	<b><math>k_h \times 10^{-5}</math> (m/s)</b>
<b>1</b>	1.82	1.82
<b>2</b>	1.46	5.69
<b>3</b>	-	3.69
<b>4</b>	1.49	2.82
<b>5</b>	68.6	93.0
<b>6</b>	-	1.41
<b>7</b>	1.21	1.00
<b>8</b>	-	-

Source: The authors (2024)

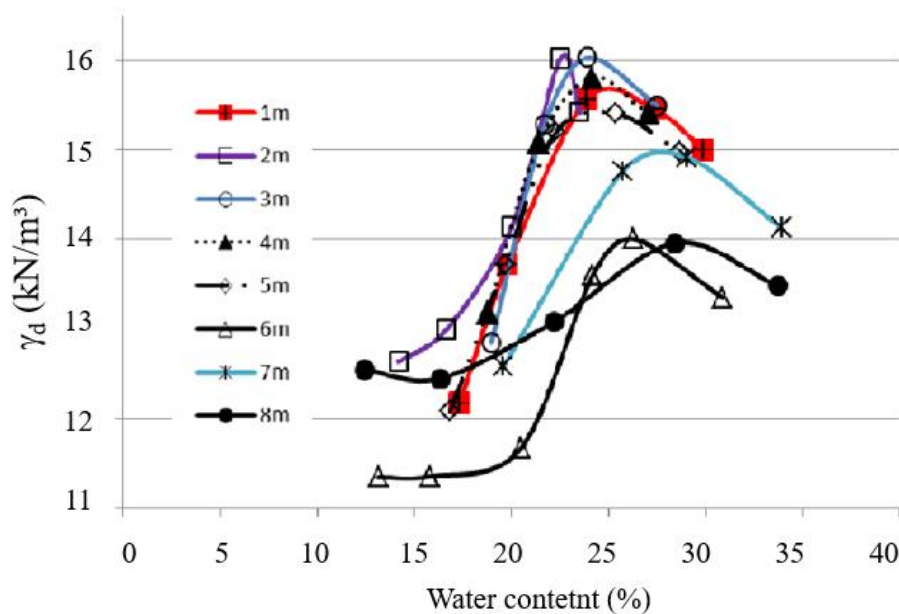
The permeability coefficient could not be obtained for depths of 3, 6, and 8 m in the vertical condition, and for 8 m in the horizontal condition, due to significant difficulties in preparing the test specimens. These difficulties resulted in the loss of a large

amount of soil during sampling, which in turn prevented the acquisition of high-quality, undisturbed samples that accurately represented the soil profile. The values of vertical hydraulic conductivity ( $k_v$ ) and horizontal hydraulic conductivity ( $k_h$ ) are on the order of  $10^{-5}$  m/s, indicating permeability typical of fine sands. This high hydraulic conductivity reflects the macroporosity of fine lateritic soils (Cozzolino and Nogami, 1993).

It was observed that there was no significant variation between the values of vertical hydraulic conductivity ( $k_v$ ) and horizontal hydraulic conductivity ( $k_h$ ). The soil exhibited a ratio of vertical to horizontal permeability coefficients of approximately 1 throughout most of the soil profile, demonstrating the isotropic nature of the soil with respect to permeability.

The soil compaction test was conducted over the entire extent of the studied profile using Standard Proctor energy. Figure 10 depicts the compaction curves determined for the test specimens.

**Figure 10** – Soil compaction curves for all depths



Source: The authors (2024)

The results of the optimal moisture content and the maximum dry unit weight of the soil obtained from the compaction test are presented in Table 8. In general, clay soils exhibit low dry densities and high optimal moisture contents. Silt soils also show low dry density values, often with well-rounded laboratory curves. High dry density and low optimal moisture content are indicative of well-graded, slightly clayey gravelly sands.

The studied soils can be described as slightly clayey silt, with an average maximum dry unit weight of 15.30 kN/m<sup>3</sup> and an optimal moisture content of around 25.6%, taking into account the usual curves of diverse Brazilian soils.

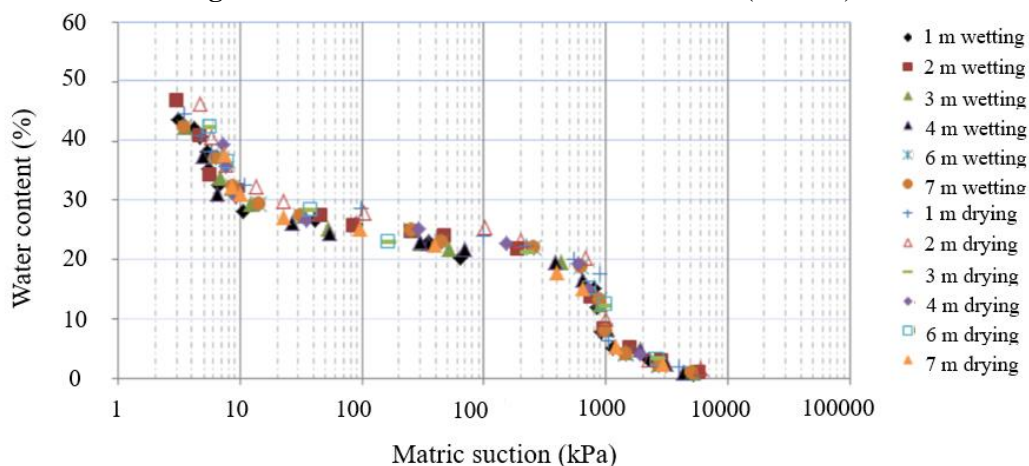
**Table 8** – Optimal moisture content and maximum dry unity weight of the soil

Depth (m)	$\gamma_d$ (kN/m <sup>3</sup> )	w <sub>opt</sub> (%)
1	15.70	24.95
2	16.10	23.90
3	16.05	24.00
4	15.81	24.16
5	15.45	24.50
6	14.04	26.10
7	14.95	28.00
8	13.98	29.00

Source: The authors (2024)

The curves obtained by the filter paper method, for both wetting and drying paths, for depths from 1 to 7 m, except for 5 m, were obtained without considering the volumetric changes experienced by the specimens during the test conduction. The equalization time adopted for the filter paper method was 7 days, as suggested by Marinho (1997), and it was applied uniformly throughout the process. Figure 11 presents the soil-water characteristic curve curves for depths of 1 m, 2 m, 3 m, 4 m, 6 m, and 7 m, obtained using the filter paper technique for both wetting and drying paths.

**Figure 11** – Soil-water characteristic curves (SWCC)



Source: The authors (2024)

The wetting and drying curves are noted to be quite similar at all depths, with closely matching values. Their bimodal shape is typical of soils with both macro and microporous structures. Both curves are consistent across all depths in terms of values and shape. The best data points obtained from the tests were used to plot the curves, enhancing the visualization of soil behavior while discarding overlapping points.

The hysteresis phenomenon was observed at some depths, although with little expressiveness. This may be caused by air bubbles trapped in the voids during wetting and/or structural alterations due to soil contraction or expansion. The analysis shows that the phenomenon is more evident at shallower depths and becomes less pronounced as depth increases. The reduced difference between the curves can be attributed to the lower void ratio of shallower samples compared to deeper ones, as indicated by the soil index properties values. Another possible explanation is a better pore distribution in the shallower depths.

## CONCLUSIONS

This study performed a comprehensive laboratory geotechnical analysis of a typical soil profile in Campinas, Brazil. This research presented relevant data, indicating the broad utility of the experimental field for various geotechnical engineering applications. Although the results are limited to the conditions of the analyses and based on a limited dataset, they allow for preliminary generalizations about overall behavior. Furthermore, they highlight the complexity of the phenomena involved in such processes. In this regard, this research has provided a better understanding of some characteristics of lateritic soil profiles. Therefore, based on the trends observed with the data and analyses, some general conclusions can be drawn:

- The characterization tests indicated that the upper soil layer is subject to surface effects and more direct weathering actions, resulting in variations in the curves of the liquid limit, plastic limit, and shrinkage limit values;
- Grain size analysis tests, conducted with and without the use of a deflocculant, revealed that clay content ranged from 0% to 50%, silt content from 25% to 45%, and sand content from 20% to 65%. Without the deflocculant, clay percentages dropped to 0% to 30%, silt increased to 25% to 65%, and sand ranged from 25% to 70%. This demonstrates the difference between field behavior and laboratory testing, as in situ soil can

be considered lateritic and thus has a structure formed by clay clods or aggregates. Under the influence of the deflocculant, the soil's granulometric classification shows a silty-clay-sandy texture up to 2 m depth, silty sand from 3 m to 8 m, and sandy-clay-silt from 8 m onwards. Without the deflocculant, the profile consists of silty-clay sand up to 2 m depth, silty sand up to 7 m, and sandy silt from 7 m to 9 m depth;

- The soil unit weight of solids is relatively high, around  $30 \text{ kN/m}^3$ , and tends to decrease with depth. This is attributed to the high iron and aluminum oxide content, further confirming the lateritic nature of the soil;
- Consolidation tests conducted with saturation at certain load levels indicated, according to Vargas's criteria (1978), that the soil is collapsible throughout its extent, with the highest collapse potential in its initial layer;
- In addition, consolidation studies presented the OCR parameter results in relation to depth, showing significant overconsolidation in the surface layers with gradual reduction with depth. This was attributed to the continuous wetting and drying process of the layers;
- Triaxial test results showed no significant variation in the soil's friction angle in the normally consolidated portions, as well as in the overconsolidated portions. However, the cohesion intercept values were relatively high, which can be explained by the significant cementation effect in these samples, along with the presence of iron oxides;
- Permeability test results indicated no significant variation between the values obtained in the vertical and horizontal directions, demonstrating the isotropic nature of the soil regarding permeability. The values of  $k_v$  and  $k_h$  were on the order of  $10^{-5} \text{ m/s}$ , indicating the permeability of fine sands and reflecting the macroporosity of fine lateritic soil structures;
- Compaction tests yielded characteristic average values of sandy silt soils;
- The soil-water characteristic curves for the studied profile were bimodal, typical of tropical soils with macro and microaggregated structures. The air entry pressure values were relatively low, similar to those obtained for sands, showing that this soil's behavior resembles that of granular soil in some aspects, such as permeability and grain size.

## ACKNOWLEDGMENTS

The first author would like to show his appreciation for the Post doctoral - PPPD program scholarship granted by the State University of Campinas (UNICAMP).

## REFERENCES

ALBUQUERQUE, P. J. R.; MIGUEL, M. G; MARQUES, R.; RODRIGUEZ, T. G.; CARVALHO, D. Estudo da resistência e colapsibilidade de um solo laterítico de Campinas. In: 13º Congresso Brasileiro de Mecânica dos Solos e Engenharia Geotécnica, Curitiba, v. 1. p. 267-272, 2006.

ASSOCIAÇÃO BRASILEIRA DE NORMAS TÉCNICAS. NBR 7181: Análise Granulométrica. Rio de Janeiro, 1984a

ASSOCIAÇÃO BRASILEIRA DE NORMAS TÉCNICAS. NBR 6459: Determinação do Limite de Liquidez. Rio de Janeiro, 1984b.

ASSOCIAÇÃO BRASILEIRA DE NORMAS TÉCNICAS. NBR 7180: Determinação do Limite de Plasticidade. Rio de Janeiro, 1984c.

ASSOCIAÇÃO BRASILEIRA DE NORMAS TÉCNICAS. NBR 6508: Determinação da Massa Específica dos Grãos. Rio de Janeiro, 1984d.

ASSOCIAÇÃO BRASILEIRA DE NORMAS TÉCNICAS. NBR 9604: Abertura de Poço e Trincheira de Inspeção em Solo, com Retirada de Amostras Deformadas e Indeformadas (procedimentos). Rio de Janeiro, 1986a.

ASSOCIAÇÃO BRASILEIRA DE NORMAS TÉCNICAS. NBR 6457: Amostras de Solos: Preparação para Ensaios de Compactação e Ensaios de Caracterização. Rio de Janeiro, 1986b.

ASSOCIAÇÃO BRASILEIRA DE NORMAS TÉCNICAS. NBR 7182: Solo - Ensaio de compactação. Rio de Janeiro, 1986c.

ASSOCIAÇÃO BRASILEIRA DE NORMAS TÉCNICAS. NBR 12007: Ensaio de adensamento unidimensional. Rio de Janeiro, 1990.

ASSOCIAÇÃO BRASILEIRA DE NORMAS TÉCNICAS. NBR 14545: Solo - Determinação do coeficiente de permeabilidade de solos argilosos a carga variável. Rio de Janeiro, 2000.

BALDOVINO, J. J. A; DE LA ROSA, Y. E. N.; FUTAI, M. M. Geomechanical Characterization of a Brazilian Experimental Site: Testing, Interpretation, and Material Properties. Applied Sciences v.14, n.13, 2024. <https://doi.org/10.3390/app14135656>

CAVALCANTE, E. H; DANZINGER, F.; GIACHETI, H. L.; COUTINHO, R. Q.; SOUZA, A.; KORMANN, A. C. M.; BELINCANTA, A.; PINTO, C. P.; BRANCO, J.M.C.B.; FERREIRA, C.V; CARVALHO, D.; ALBUQUERQUE, P. J. R. Campos Experimentais Brasileiros. Geotecnia (Lisboa), v. 111, p. 99-205, 2007.

CHANDLER, R.J.; CRILLY, M. S.; MONTGOMERY-SMITH, G.A low-cost method of assessing clay desiccation for low-rise buildings. In: Proceedings of the Institute Civil Engineers, v.92, p.82-89, 1992.

CORTIZO, P. T.; ALBUQUERQUE, P. J. R.; RODRIGUEZ, Tiago Garcia. Estudo do comportamento mecânico de um solo de diabásio da região de Campinas nas condições saturada e não saturada. In: 7º Simpósio Brasileiro de Solos Não Saturados, v. 1, p. 127- 132, 2011.

COZZOLINO, V. M. N.; NOGAMI, J. S. Classificação geotécnica MCT para solos tropicais. Solos e Rochas, v. 16, p.77-91, 1993.

DOS SANTOS, J.C; COUTINHO, R.Q. Geological and Geotechnical Characterization of Soils from the Barreiras Formation in a Subarea of Study in Maceio, Alagoas State, Brazil. Geotech Geol Eng, v. 41, p. 107-133, 2023. <https://doi.org/10.1007/s10706-022-02266-8>

GARCIA, J. R.; ALBUQUERQUE, P. J. R. Analysis of the contribution of the block-soil contact in piled foundations. Latin American Journal of Solids and Structures, v.16, n.6, p.1-22, 2019. <https://doi.org/10.1590/1679-78255565>

GON, F.S. Caracterização geotécnica através de ensaios de laboratório de um solo de diabásio da região de Campinas/SP. Dissertação de Mestrado. Faculdade de Engenharia Civil, Arquitetura e Urbanismo, Universidade Estadual de Campinas, Brasil, 2011.

JENNINGS, J. E.; KNIGHT, K. A Guide to Construction on or with Materials Exhibiting Additional Settlement due to a Collapse of Grain Structure. In: Proceedings of 4<sup>th</sup> Regional Conference for African on Soil Mech. Found. Eng., Durban, p. 99-105, 1975.

HEAD, K. H. Manual of Soil Laboratory Testing vol III. John Wiley & Sons, 3 ed, 496p, 1986.

MARINHO, F.A.M.; PINTO, C.S. Evaluation of pore size characteristic of plastic soils. In: 3º Simpósio de Solos Não Saturados, Rio de Janeiro, vol. 1, p. 1-11, 1997.

MOURA, A. S.; RAMOS, M. R.; JUNIOR, E. C.; FILHO, F. P. L.; MENEZES, P. H. L. B. Caracterização preliminar geotécnica do subsolo do Campo Experimental de Geotecnia e de Fundações da Universidade Federal do Ceará (CEGEF – UFC). Brazilian Journal of Development, v.7, n.4, p. 33781–33796, 2021. <https://doi.org/10.34117/bjdv7n4-028>

ROCHA, B. P.; GIACHETI, H. L. Site characterization of a tropical soil by in situ tests. Dyna, v. 85, n. 206, p. 211-219, 2018. <https://doi.org/10.15446/dyna.v85n206.67891>.

VARGAS, M. Introdução à Mecânica dos Solos. McGraw-Hill do Brasil, 1 ed, 450p, 1978.

ZUQUETTE, L.V. Análise crítica da cartografia geotécnica e proposta metodológica para condições brasileiras. Tese de Doutorado. Escola de Engenharia de São Carlos, Universidade de São Paulo, Brasil, 1987.